ABUAD Journal of Engineering and Applied Sciences (AJEAS)

ISSN: 2992-5584

Volume 2, Issue 1, 10-19

# Appraisal of the Propping Potential of Luwa Sand in Nigeria for Hydraulic Fracturing Applications

Roy Zwalatha MILTON [1*], Mohammed Bello ADAMU [1], Kabir GARBA [2], Saidu Mohammed SALEH[1], Adamu Yahaya YAKUBU[1]

[1]*Department of Petroleum Engineering, Abubakar Tafawa Balewa University, Bauchi, Bauchi State, Nigeria*
[2]*Department of Chemical Engineering, Abubakar Tafawa Balewa University, Bauchi, Bauchi State, Nigeria*

*Correspondence: rmzwalatha.pg@atbu.edu.ng; Tel.: +2348140673525

*Date Submitted:* 25/12/2023
*Date Accepted:* 18/02/2024
*Date Published:* 30/06/2024

***Abstract***: *Natural sands made of spherical and round grains are widely used as proppants during hydraulic fracturing to increase recovery rate of hydrocarbon production. Synthetic proppants with high crush strength are employed for deep reservoir fracturing; however, this type of proppants suffer the disadvantages of high density, high cost and pose environmental hazards. This research was conducted with the aim to assess sands collected from Luwa River in Toro, Bauchi state of Nigeria for possible use as natural sand proppants. An epoxy resin-coated sand was produced using a simple method to modify the sands' properties. A series of experiments were conducted in accordance with API recommended practice to determine the propping potential of the sand and the resin coated sand. The result from sieve analysis of 20/40 mesh size of Luwa sand revealed a mean size of 625.2 microns (0.625 mm). An X-ray fluorescence (XRF) result showed the presence of aluminosilicates ($Al_2O_3$ and $SiO_2$) composition in Luwa sands. The sands recorded a hardness of 8 on the Mohs scale. Analysis of the shape parameters for sphericity and roundness was 0.8 and 0.8 (Krumbein-Sloss) respectively; it has bulk density of 1.64 g/cm$^3$, acid solubility of 0.7% and 4.32% for the resin-coated sand. The sand has turbidity value of 28.98 NTU, loss on ignition in the range of 1.33% to 1.64% and crush resistance varies between 2000-3000 psi for Luwa sand and 4000-5000 psi for the coated sand. A comparison of the experimental results with API standard and conventional Ottawa and Brady models showed the sand competes favourably with these standards in all parameters for consideration as a proppant except for the crush resistance where more than 10% fragments was generated at low pressure of 3000 psi. However, the sand can be applied in shallow depth reservoirs.*

***Keywords:*** Hydraulic fracturing, proppants, luwa sand, crush resistance, resin-coated sand.

## 1. INTRODUCTION

Unconventional oil and gas reservoirs characterized by poor rock permeability hold sufficient quantity of hydrocarbons (Liu *et al*., 2018). Hydrocarbon resources from these reservoirs represent the main global future energy reserves, and thus has led to the increased demand for exploration and production techniques to ensure utilization of these resources. In order to effectively produce hydrocarbon resources from unconventional reservoirs, there is the need to employ stimulation measures aimed to create a connection of fracture networks within the reservoir formation. The purpose of hydraulic fracturing is to create a highly conductive channel connecting the reservoir formation with the wellbore, increase contact area and ultimately maximize production (Zheng *et al.*, 2017; Al-Rbeawi, 2017).

The success of hydraulic fracture conductivity depends on properties of the selected proppant, especially the shape of the grain material (Mehmood *et al*., 2022). Mehmood *et al*. (2022) carried out research to investigate the effect of using rod-shaped proppants on the conductivity of hydraulic fractures. The high conductivity achieved as a result of high values of porosity and permeability was attributed to the cylindrical shape of this proppant. In order to determine the effect of different proppant shapes on the performance of hydraulic fractures, a model was implemented in FLAC3Dplus -TMVOC software. The results have shown that when rod-shape proppant with aspect ratio of 1 and the same diameter as spherical proppants is used, hydrocarbon recovery can be improved by up to 7%. However, when the size of the rod-shape proppant is increased from an aspect ratio of 1-10, the gas recovery was improved by 13%, but significant proppant deformation was recorded (Mehmood *et al*., 2022).

The choice of proppants greatly affects the physical success and economic optimization of hydraulic fracturing treatment. During a hydraulic fracturing operation, 100 to 500 tons and infrequently up to 1500 tons of proppant are used (Conway *et al*., 2007). The expense of the propping agent alone could be as high as 67% of the total stimulation costs; this has given proppants the attention as a crucial parameter for technological research (Zoveidavianpoor *et al.*, 2014).

Choosing a suitable proppant for hydraulic fracturing is an important design choice to optimize the production of oil and natural gas from reservoirs (Liang *et al.*, 2016). Proppants are selected based on the requirements that they are permeable and strong enough to prop hydraulic fractures open without being crushed (Khair *et al.*, 2017). Proppants can be natural materials (sand grains) or artificially engineered (Resin-coated sand and Ceramic). These materials are common propping agents used in the oil and gas industry.

Over the years, several materials have been characterised and explored as potential proppants by different researchers. The work of Abu Bakar *et al*. (2018) showed the successful characterization and improvement of beach sand using simple polyurethane coating formulated from palm oil-based polyols. Although the crush resistance of the sand was low, the coated sand showed good resistance to acid solubility and could withstand 4000 psi applied pressure before more than 10% crushed fines was generated (Abu Bakar *et al*., 2018).

Bandara *et al*. (2022) studied proppant crushing and embedment using calibrated discrete element models. Results from their study revealed that the choice of a suitable proppant based on reservoir type is an important step to quantifying the extent of proppant crushing and embedment within hydraulically-induced fractures (Bandara *et al*., 2022).

For Elochukwu and Kiat (2020), two sands from Malaysia were characterized as viable proppants for use in hydraulic fracturing. X-ray diffraction (XRD) analysis show that both sands are composed of quartz and metal oxides. The result for the crush resistance test showed that one of the sands was strong to withstand 4000 psi pressure without generating more than 10% crushed particles, whereas the other sand showed better strength and could resist 8000 psi pressure without generating more than 10% fines. A high acid solubility value was recorded for the sands when set side by side with commercial sand proppants. The authors attributed the high value to be an indication of soluble metal oxides as confirmed by the XRD analysis (Elochukwu and Kiat 2020).

Labus *et al*. (2022) proposed a novel coke-based proppant to be used in the fracturing of coal seams for the production of coalbed methane. The idea is based on the assumption that the new proppant when introduced will be more effective than conventional proppants used in hydraulic fracturing. The authors identified samples of coke that satisfies the specification of propping grains. The shape parameters of coke materials were investigated for applications in the synthesis of anodic electrodes. However, the authors suggest the need to examine the sphericity and roundness of this material for possible use as proppants (Labus *et al*., 2022). It is evident from literatures that coke grains have a bulk density value of 0.7 -1.1 g/cm$^3$, while the compressive strength is assumed to be in the range of 1500-3000 psi (Labus *et al*., 2022). Consequently, the low bulk density of coke will make it easy for its transportation with fracturing fluids without necessarily settling before it gets to the tip of hydraulic fractures. Although the low crushing rate recorded in the study will limit the application of coke to shallow reservoirs.

In the study to characterise Malaysian sands for possible use as proppant, X-Ray fluorescence (XRF) analysis was carried out on two sand samples and a commercial proppant. The commercial proppant showed high percentage composition (49.46%) of aluminium oxide ($Al_2O_3$), an additive used to increase the strength of minerals (Ismail *et al*., 2011). Crush resistance tests on the three samples revealed that the commercial proppant produced 8.26% fines at a confined pressure of 2500 psi and more than 10% fines at the pressure of 3000 psi. However, the other samples with small amounts of $Al_2O_3$ (5.30% - 5.73%) produced more than 23% fines at the pressure of 2500 psi and more than 10% fines at a lower pressure of 1500 psi, indicating low strength compared to the commercial proppant with high composition of $Al_2O_3$.

Series of experiments were carried by Sun *et al*. (2022) using quartz sand and ceramic proppants obtained from Changqing oilfield China. The response of fracture conductivity at different proppant mixing ratios was evaluated. The selection of widely used 20/40 mesh quartz sand, 20/40 mesh ceramic, 40/70 mesh quartz and 40/70 mesh size ceramic were used for the study. In their experiments, seven closure stress measurement was recorded for the tests. The results showed that conductivity value increases with increasing proppant size, while the conductivity of ceramic proppants is greater than that of quartz sand of the same particle size.

The physical and chemical composition of three sand samples from a desert in Sudan was evaluated for parameters that qualify the sands as proppant (Khair *et al.*, 2017). The results show favourable potential when compared with the API standard as all values are within acceptable limits; although the crush strength of the sand is low, implying the sands can only be applied in reservoirs with low closure stress of 2000 psi, otherwise the sands need reinforcement for application in deeper reservoirs (Khair *et al*., 2017).

In order to investigate the effect of temperature and type of proppants on the dissolution of ceramic and quartz proppants, Xu *et al*. (2022) immersed a 20/40 mesh size of the two proppants in mud acid at 65 ºC and 85 ºC for 30 minutes. They found out that the acid solubility of the proppants increases greatly with temperature. The solubility of the ceramic proppant was significantly higher than the quartz sand under the same test conditions. The high solubility of the ceramic proppants was attributed to the composition of clay minerals in bauxite (the main component of ceramic proppants) which are susceptible to attacks by HF acid. Whereas the quartz sand composed of silica does not react with HCl in mud acid (Xu *et al*., 2022).

The major setback with the use of natural sand proppant has been its susceptibility to crushing and fines generation at low pressures. However, natural sands with low crush resistance are recommended for coating with resin to form a resin-coated proppant which is stronger than the original sand. Figure 1 shows the response of natural sand and resin-coated sand to increasing closure stress.

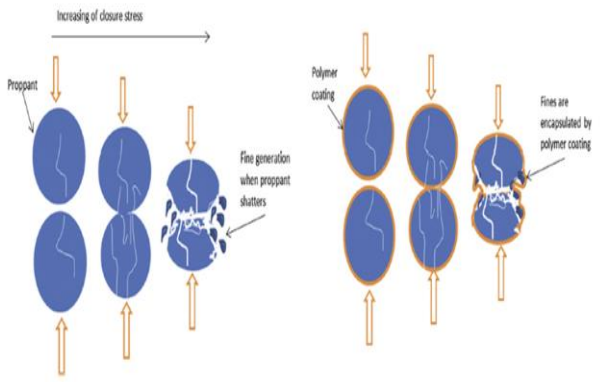


Figure 1: The response of uncoated (left) and coated (right) proppants to closure stress (Stevens, 2014)

The development of deep reservoirs, with high closure pressures of up to 20,000 psi has posed a big challenge for the petroleum industry as conventional sand proppants do not provide sufficient fracture conductivity (Palisch *et al.*, 2015). This led to the introduction of synthetic ceramic proppants targeted at providing improved conductivity and above all, the productivity of the well and also, the recovery of hydrocarbon resources under a wide range of reservoir conditions (Palisch, 2013). Figure 2 shows the three main types of proppants used in hydraulic fracturing.

(a) (b) (c)

Figure 2: Proppant types: (a) natural sand (b) resin-coated sand (c) ceramic proppant

The toughness of a proppant has been regarded as the most important physical requirement of the material necessary to withstand the pressure exerted by the closure stress on proppant grains (Zheng, 2017). The ability to withstand crushing from overburden pressure is an indication of the strength of a proppant (Zoveidavianpoor and Gharibi, 2016; Mocciaro *et al.*, 2018).

Resin coated sand and ceramic proppants are known to endure higher closure stresses due to the high breakage resistance of these proppants (Palisch *et al.*, 2014; Kaufman *et al.*, 2015). Low bulk density is considered when selecting a proppant, because this property permits an easy flow of proppants in fracturing fluid thereby preventing them from unequal dispersal and build-up within fractures (Gu *et al.*, 2015).

Proppants are subjected to immersion in mud acids to determine the amount of undesirable soluble materials present in the proppant. This procedure is performed to decide the suitability of a proppant in conditions of contacts with acids. Low turbidity means proppant has small amount of impurities suspended on its surface. When in high amount, these foreign particles can plug the pore throats of proppants and consequently, restrict the flow of hydrocarbons from induced fractures to the wellbore.

Some authors reported the existence of a relationship between proppant type, particle size and crush resistance such that small sized particles tend to have high crush strengths than particles with large size. However, larger particles are thought to produce bigger fractures (Zheng, 2017; Tang *et al.*, 2018). There are studies that recorded success-using mixture of different size of proppant to provide better fracture conductivity than proppants with uniform size; however, the addition of small sized proppants in the mixture decreases the void ratio, and subsequently reduces permeability and overall fracture networks (Guo *et al.*, 2012; Zheng, 2017).

The sphericity of proppants measures how closely the shape of the grains resembles that of a perfect sphere and the roundness measures the sharpness of the corners and edges of the grains. The sphericity and roundness of proppants significantly affect the grain packing in hydraulic fractures.

This study was carried out to characterize Luwa sand deposits in Nigeria for possible application as proppants in the oil and gas industry. The physical and chemical parameters of the sand were determined to find its suitability based on the American Petroleum Institute (API) and the International Organisation for Standardization (ISO) standards. The crush resistance of proppants which is the most important parameter that qualifies a proppant for use in hydraulic fracturing was the main focus of the study. The resin coating on the sand was done to improve the strength of the sand for use in hydraulic fracturing of deep formations.

The challenge with the application of natural sand proppants is that they tend to be ineffective in deep reservoirs with high closure stress. Natural sands have low strength compared to resin-coated sand and ceramics. However, resin-coated sand and ceramics are more expensive to use, considering the high cost of production and the costly fracturing fluid additives required to transport these materials to the tip of hydraulic fractures. This has made natural sand proppants to be the most sort after proppant, because of its availability, low cost and the low density which makes it easy to be transported by fracturing fluids.

## 2. MATERIALS AND METHODS

### 2.1 Study Area

The sand used for this study was sourced from Toro local government area of Bauchi State in Nigeria at latitude 10˚4’48” N and longitude 9˚9’40” E with a climate type of tropical Savanna, wet. Luwa river is host to the Luwa sand used for this experimental study. The occurrence of the sand dune was studied and three representative sand samples were collected for laboratory study shown in Figure 3.

https://doi.org/10.53982/ajeas.2024.0201.02-j

Figure 3: (a) Site of sand deposit in Luwa river (b) Luwa sand sample used for this study

**2.2 Sample Preparation**

The sand sample was weighed with a digital weighing balance prior to washing in order to remove fine impurities grain and contaminants. The loss of contaminants (measured in percent) was determined by comparing the original sand weight and the washed sand weight. The exploratory analysis of Luwa sand for the determination of its suitability as a proppant involved application of the standard American Petroleum Institute (API) recommended practice (RP) 19C (also ISO 13503-2).

**2.3 Sieve Analysis**

Sieve analysis was used to determine the particle size distribution of Luwa sand. The test was carried out on the dried sample of the sand after washing the sand to remove impurities. For the 20/40 US mesh size designation used in this study, the sieves 16, 20, 30, 35, 40 and 50 were arranged in a decreasing order of sieve openings. The mass retained on each of the sieves was recorded as reported in Figure 5 and the percentages of the mass retained plotted in Figure 6 were calculated to plot the particle size distribution curve of the 20/40 mesh size sand in Figure 7.

**2.4 Turbidity Test**

The test for turbidity was performed to determine the amount of suspended particles present in the sand. The test was carried out on the sand prior to washing and after sieve analysis. 100 ml of demineralized water was added to 70 g of sand in a 250 ml flask. The sand was allowed to stand in the water for 30 minutes. A shaker bottle with the frequency set to 7 was used to shake sand and water mixture for 30 seconds. The flask was removed from the shaker bottle and allowed to stand for 5 minutes. 25 ml of the water and silt suspension was removed using a syringe. The suspended-particle sample was placed in a test vial and placed in a calibrated turbidimeter. The sample turbidity was recorded in Nephelometric turbidity unit (NTU).

**2.5 X-Ray Fluorescence (XRF) Test**

XRF measurements were carried out on the three representative samples of Luwa sand using Rigaku's Supermini 200 wavelength dispersive X-ray fluorescence spectrometer under helium (He) atmosphere. A palladium (Pd) X-ray tube at a voltage of 60 kV and current 10 µA with 10 mm beam spot size, and silicon (Si) drift detector comprised of Peltier electronic circuit cooling system was used. The elemental detection limits were from low parts-per-million (ppm) to high weight percent (%wt.). The analytical uncertainties were generally within 0.1-1% (RSD).

**2.6 Hardness Test**

The Mohs hardness scale was used to test for the relative resistance of Luwa sand to scratching. The mineral that could not be scratched by Luwa sand was deemed to have the same hardness value as Luwa sand. On the Mohs scale, Talc has a hardness value of 1, Gypsum 2, Calcite 3, Fluorite 4, Apatite 5, Orthoclase 6, Quartz 7, Topaz 8, Corundum 9 and Diamond 10 in an order of increasing hardness value.

**2.7 Sphericity and Roundness Test**

The shape of the 20/40 mesh size sand was evaluated by visual estimation with the aid a microscope and the Krumbein-Sloss chart. The sphericity and roundness of the sand was determined using twenty (20) grains of the sand randomly selected for the test. Each particle of the sand was evaluated visually by magnification of the microscope as recommended by API RP 19C. The shapes of the individual grains observed were compared to the shapes on the chart and the corresponding value was recorded as grain sphericity and roundness.

**2.8 Bulk Density Test**

A weighing balance and a calibrated cylinder of 600 $cm^3$ were used to evaluate the bulk density of the sand. The bulk density of the sand was calculated using Equation (1).

$$\rho = m_s / V_{cyl} \tag{1}$$

Where,
$m_s$ is the mass of the sand
$V_{cyl}$ is the volume of the cylinder

**2.9 Acid Solubility Test**

Standard acid solubility was conducted on the sand. The solubility of the sand in acid was measured by comparing the change in weight after submerging 5 g of the sand in a 100 ml solution of a mixture of 12% hydrochloric acid (HCl) and 3% hydrofluoric acid (HF). Prior to this procedure, the sand to be used for the test was dried in an oven at a temperature of 105 °C. 5 g of sand was dropped in 100 ml mixture HCl/HF acids and the slurry was kept in the oven set at the temperature of 66 °C for 30 minutes. The acid solubility of Luwa sand and the resin-coated sand was calculated using Equation (2).

$$\text{Acid solubility, S (\%)} = \left(\frac{(m_s + (m_{fs} - m_f)}{m_s}\right) \times 100 \tag{2}$$

**2.10 Loss on Ignition (LOI) Test**

Three representative samples code-named; LS 01, LS 02 and LS 03 were weighed and their masses recorded. The samples were subjected to heating at 900 °C in a furnace. After 4 hours, the samples were allowed to cool and their individual masses was recorded. The mass loss from each of the sample indicates the amount of ignitable materials on the sand. The loss on ignition (measured in %) is recorded using Equation (3).

$$\Delta m_{LOI} = (m_s - m_f)/m_s \times 100 \quad (3)$$

Where, $\Delta m_{LOI}$ is the loss on ignition expressed in percent (%)
$m_s$ is the mass of the sand before firing expressed in grams
$m_f$ is the mass of the sand after firing expressed in grams

### 2.11 Resin Coating of Luwa Sand

A resin-coated proppant was produced from Luwa sand and Diglycidyl ether of bisphenol-A (DGEBA) E-51 epoxy resin and an epoxy hardener using a simple method adopted from US patent US11396625B2. The sand was washed and allowed to dry. The epoxy resin and hardener were measured and mixed in the ratio 3:1 respectively using a measuring cup. The mixture was stirred vigorously using wooden sticks, a dropper was used to drop the mixture on the sand. The slurry of the sand and epoxy resin was then mixed to ensure the epoxy encapsulates the whole of the sand. When the epoxy resin and sand mixture was about to set, the individual grain with the resin coating were transferred to a plane surface and allowed to cure for 24 hours at room temperature of 26 °C.

### 2.12 Crush Resistance Test

In the crush resistance determination procedure, the sand was exposed to different level of stress and the amount of crushed sand particles was recorded in weight percent. The sand for the test was measured and packed into a test cell such that the sand surface in the test cell is level. Crush resistance was conducted using an analogue TUN-1000 (1000 kN) universal testing machine. The procedure was conducted in triplicates and the average percentage of fines was computed. The steps were repeated at stress levels of 1000 psi, 2000 psi, and stopped at 3000 psi where greater than 10% of Luwa sand were crushed to produced fragments that were finer than the 50 mesh size sieve in the 20/40 mesh size arrangements. For the resin-coated sand, the same steps were repeated at stress levels of 1000 psi, 2000 psi, 3000 psi, 4000 psi and stopped at 5000 psi for the same reason as with the procedure for Luwa sand.

## 3. RESULTS AND DISCUSSIONS

### 3.1 Sieve Analysis

The particle size distribution of 20/40 mesh size Luwa sand is 100% as all particles are retained between the primary sieve (Mesh No. 20 corresponding to 0.850 mm) and the secondary sieve (Mesh No. 40 corresponding to 0.425 mm). This result conforms with the API requirement that a minimum of 90% of proppants must pass the coarse sieve and be retained on or above the fine sieve (API RP 19C). The result can be compared to that obtained from the work of Kamel *et al*. (2019) where the 20/40 mesh quarry sand fail to meet this requirement as 76.67% mass fraction was reported. However, the 40/70 mesh quarry sand met the requirement with over 90% mass recorded (Kamel *et al*., 2019). Figures 5, 6 and 7 show the sieve analysis parameters of 20/40 mesh size Luwa sand.

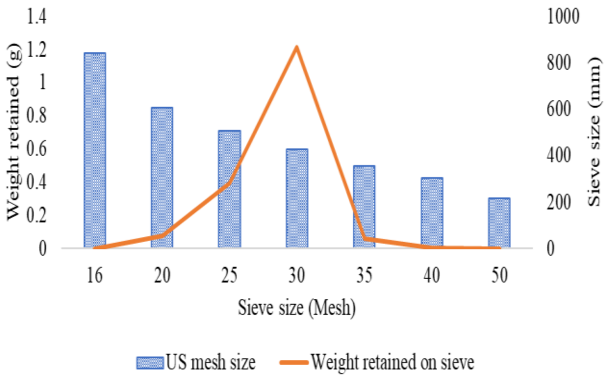


Figure 5: Result for the weight retained on 20/40 mesh Luwa sand

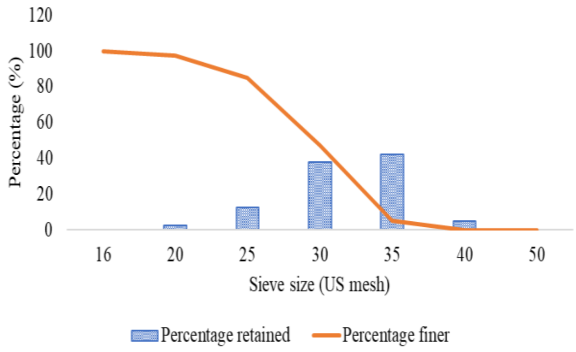


Figure 6: Result for the percentage retained and percentage finer

The particle size distribution curve of 20/40 mesh Luwa sand shows it is uniformly graded based on the analysis of the effective size and the coefficients of uniformity and gradation parameters of the sand.

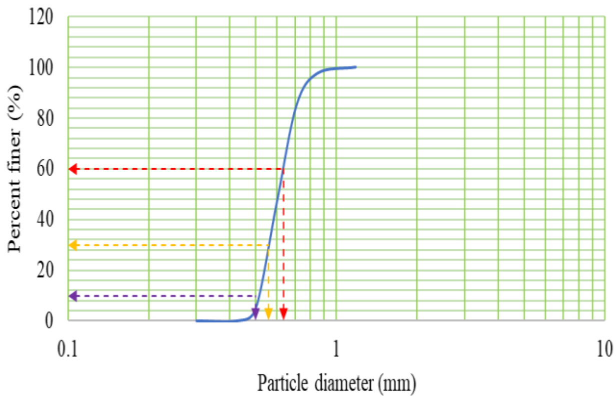


Figure 7: The particle size distribution curve

From the particle size distribution curve, the effective size is the diameter corresponding to 10% finer, or simply

$D_{10}$. The uniformity coefficient is determined by the relation in Equation (4):

$$C_u = D_{60}/D_{10} \quad (4)$$

Where $C_u$, is the uniformity coefficient and $D_{60}$ is the diameter corresponding to 60% finer in the particle size distribution curve.

The coefficient of gradation is determined by the relation in Equation (5):

$$C_c = D_{30}^2/(D_{60} \times D_{10}) \quad (5)$$

Where $C_c$, is the coefficient of gradation and $D_{30}$ is the diameter corresponding to 30% finer.

Table 1 shows the effective size and the coefficients of uniformity and gradation of 20/40 mesh Luwa sand.

Table 1: Effective size, coefficients of uniformity and gradation results

| 10% finer $D_{10}$ (mm) | 30% finer $D_{30}$ (mm) | 60% finer $D_{60}$ (mm) | Uniformity coefficient $C_u$ | Coefficient of gradation $C_c$ |
|---|---|---|---|---|
| 0.50 | 0.56 | 0.64 | 1.28 | 0.98 |

The parameters for determination of the mean diameter of Luwa sand are expressed in Table 2.

Table 2: Parameters for mean diameter evaluation

| US mesh size | Mid-size $d$ (μm) | Frequency of occurrence $n$ (% by mass) | $n.d$ |
|---|---|---|---|
| 12 to 16 | 1440 | 0 | 0 |
| 16 to 20 | 1015 | 2.4 | 2436 |
| 20 to 25 | 780 | 12.4 | 9672 |
| 25 to 30 | 655 | 38.0 | 24890 |
| 30 to 35 | 550 | 42.2 | 23210 |
| 35 to 40 | 462.5 | 5.0 | 2312.5 |
| 40 to 50 | 362.5 | 0.0 | 108.75 |
| | Total | 100 | 62520.50 |

The mean diameter ($d_{av}$) of 20/40 mesh size Luwa sand is evaluated using Equation (6):

$$d_{av} = \frac{\sum n.d}{\sum n} \quad (6)$$

The mean diameter of the sand $= 625.2\ \mu m = 0.625\ mm = 0.025$ in.

where, in is the unit of the mean diameter in inches.

**3.2 X-Ray Fluorescence (XRF)**

The result of the major oxide composition of Luwa sand is shown in Table 3. The sand is mainly composed of aluminium oxide ($Al_2O_3$) and silicon oxide ($SiO_2$). The $Al_2O_3$ content is higher in samples A and B, however, sample C has a slightly higher composition of $SiO_2$. The XRF results for samples A and B come close to the XRD result for the commercial proppant in the work of Ismail *et al.* (2011). While corundum is suspected to be the form of $Al_2O_3$ in Luwa sand due to the crystalline nature of the sand, mullite is reported to be responsible for the composition of $Al_2O_3$ in the commercial proppant (Ismail *et al*., 2011). The proportion of the composition of aluminosilicates in Luwa sand can be compared with that composition in the synthesized lightweight ceramic proppants, implying improved strength in Luwa sand over silica-based sands.

Table 3: X-ray fluorescence (XRF) result

| Oxides | Composition (%) | | |
|---|---|---|---|
| | Luwa sand A | Luwa sand B | Luwa sand C |
| $SiO_2$ | 45.6% | 44.7% | 29.85% |
| $Al_2O_3$ | 53.0% | 49.6% | 29.37% |
| $Fe_2O_3$ | 0.61% | 1.43% | 0.06% |
| CaO | 0.152% | 0.35% | 0.07% |
| MgO | 0.00% | 0.00% | 2.83% |
| MnO | 0.07% | 0.23% | 0.01% |
| $K_2O$ | 0.36% | 0.00% | 0.06% |
| $P_2O_5$ | 0.08% | 0.09% | 0.10% |
| $TiO_2$ | 0.00% | 0.53% | 0.02% |

**3.3 Hardness**

The hardness of the samples of Luwa sand was determined to be 8. This value is high when compared to the 6.90 reported for the Wadi Qena samples in the work of Wahab *et al*. (2022). Although the authors used the Lm500 hardness tester to determine the hardness value of the sands, the difference in the values for Luwa sand and the Wadi Qena samples is likely due to the high composition of the crystalline form of aluminium oxide (corundum) in Luwa sand and the relatively low composition of the mineral in the Wadi Qena sands (composed mainly of silicon oxide).

**3.4 Sphericity and Roundness**

The sphericity of Luwa sand is 0.8, and the roundness is also 0.8 (Krumbein-Sloss chart). The average of the individual grain values (Figure 8) from the chart was computed as the sphericity and roundness of the sand. These values satisfy the API requirement with the sphericity and roundness values of greater than 0.6.

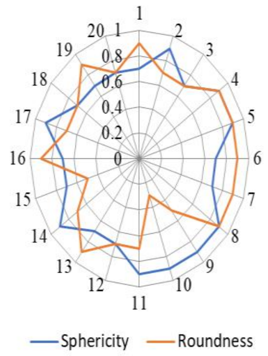


Figure 8: Sphericity and roundness result

### 3.5 Turbidity

The turbidity of Luwa sand is presented in Figure 9. The sand recorded a low amount of suspended particles when compared with the 246 FTU reported for a commercial proppant in the study by Ismail *et al*. (2011). However, the sand samples in the study has a slightly low turbidity than the commercial proppant but still significantly higher than that of Luwa sand (Ismail *et al*., 2011). The turbidity of Luwa sand is within the accepted limit set by API (< 250 NTU).

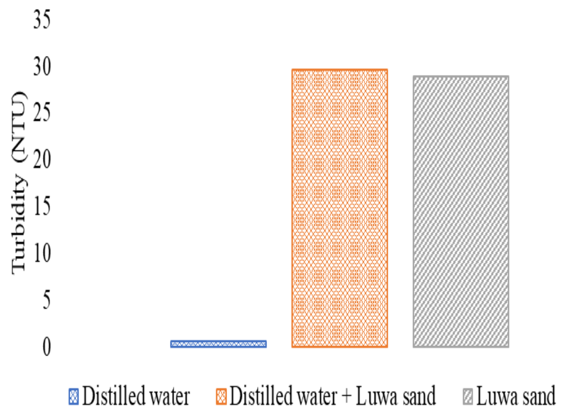


Figure 9: Turbidity result

### 3.6 Bulk Density

A value of 1.64 $g/cm^3$ was recorded as the bulk density of Luwa sand as presented in table 4. Although the value is a bit high when compared with Ottawa (1.54 g/cm$^3$) and Brady (1.57 g/cm$^3$) sand models (Ismail *et al*., 2011). However, the value is within the API limit (< 2 g/cm$^3$). Proppants with high bulk densities are not easily transported with fracturing fluids. These proppants are prone to settle in the wellbore even before reaching into hydraulic fractures.

Table 4: Bulk density results

| Sample No. | Bulk Mass ($M_s$) (g) | Bulk Volume ($V_{cyl}$) (cm$^3$) | Bulk density ($M_s/V_{cyl}$) (g/cm$^3$) |
|---|---|---|---|
| 1 | 984 | 600 | 1.64 |

### 3.7 Acid Solubility

The acid solubility result for 20/40 mesh Luwa sand and the resin-coated sand is presented in Table 5. The value obtained from the resistance test show that Luwa sand is not readily soluble in mud acid. This could be compared to the high values reported in the work by Elochukwu and Kiat (2020). The authors suggested that the high solubility of the sands in mud acid was due to the significant content of metal oxides ($Fe_2O_3$ and ZnO) in the sands (Elochukwu and Kiat 2020). Whereas these sands have high solubility value when compared with Luwa sand, the resin-coated Luwa sand has high solubility value than the Baram and Tanjung sands used in the work of Elochukwu and Kiat (2020). Nonetheless, the solubility of Luwa sand, the resin-coated sand and the Baram and Tanjung sands are within API acceptable limit.

Table 5: Acid solubility results

| Sample No. | Weight before (g) | Weight after (g) | Solubility (%) |
|---|---|---|---|
| Luwa sand | 5 | 4.965 | 0.7 |
| Resin-coated sand | 5 | 4.784 | 4.32 |

### 3.8 Loss on Ignition

The loss on ignition test result for Luwa sands is shown in figure 10. The loss on ignition of the sands is high when compared to the values obtained for the sands used in the study by Wahab and Ibrahim (2021). This variation could be due to the difference in the elemental composition of the sand samples in the study when compared with Luwa sand (Wahab and Ibrahim 2021).

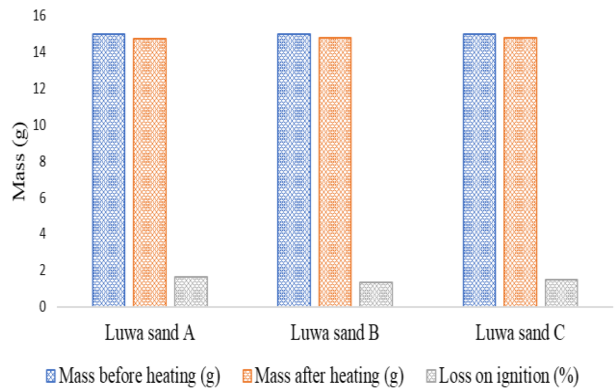


Figure 10: Loss on ignition result

### 3.8 Crush Resistance

The percentages of sand crushed at different stress level for 20/40 mesh Luwa sand and the resin-coated sand are presented in figure 12 and 13 respectively. The crush resistance of the sand is in the same range as that of the commercial proppant sample used in the work of Ismail *et al*. (2011). In their work, where the aluminosilicate commercial proppant produced more than 10% crushed fines at the pressure of 3000 psi, the silica-based sands produced more than 10% fines at lower pressures of 1500 psi (Ismail *et al*., 2011). The resin coating on Luwa sand has succeeded in reducing the amount of fines produced due to crushing of the sand by applied pressure. Where more than 10% of fragments was produced at 3000 psi in the test for the sand, this amount was produced when a higher pressure of 5000 psi was applied for the resin-coated sands.

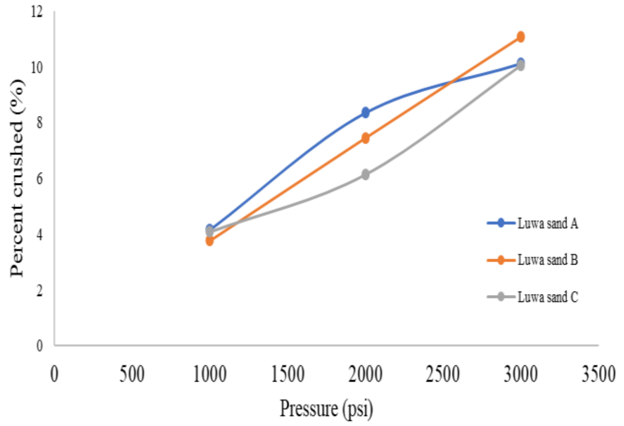


Figure 11: Crush resistance result for 20/40 mesh size Luwa sand

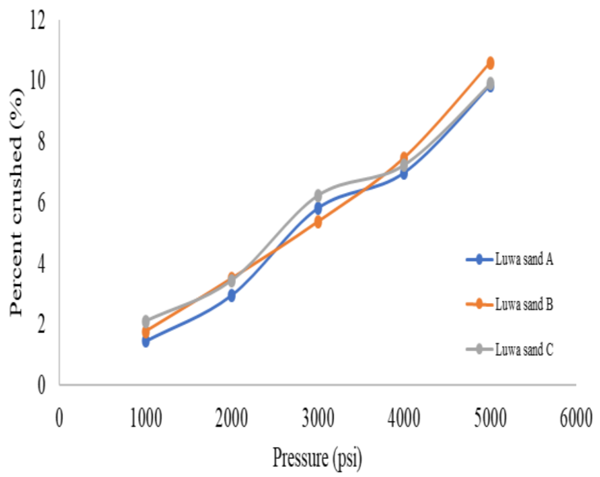


Figure 12: Crush resistance result for resin-coated sand

Table 6 contains a summary of the properties of Luwa Sand determined from experimental procedures based on the American Petroleum Institute recommended practice (API RP 19C) and the International Organisation for Standardization (ISO 13503-2).

Table 6: Summary of results

| PROPERTY | RESULT | API/ISO STANDARD |
|---|---|---|
| Particle size distribution | 100 % | 90 % within specified size ranges e.g. 20/40 (850 – 425 µm) |
| Mean particle diameter | 625.2 µm, 0.625 mm | N/A |
| Roundness | 0.8 | ≥ 0.6 |
| Sphericity | 0.8 | ≥ 0.6 |
| Turbidity | 28.98 NTU | < 250 NTU |
| Bulk density | 1.64 g/cm$^3$ | < 2.0 g/cm$^3$ |
| Acid solubility | 0.7 % for Luwa sand and 4.32% for resin-coated sand | < 2 % |
| Crush resistance | 2 K value (< 10 % at 2000 psi) for Luwa sand<br>4 K value (< 10% at 4000 psi) for resin coated sand | < 10 % fines |

## 4. CONCLUSION

The investigation into the properties of Luwa sand in Nigeria showed that the sand has all the necessary qualities for consideration as a commercial proppant in hydraulic fracturing applications. However, the use of the sand might be limited to reservoirs with 2000 psi closure stress as the crush resistance result produced more than 10% fines on the average of the three sand samples at 3000 psi. Nonetheless, for reservoirs where closure stress exceeds 2000 psi, the sand is recommended for coating with resin to form a stronger resin-coated. The resin-coated sand in this study shows the ability to withstand a closure stress of up to 4000 psi, implying more strength than the original sand. The sieve analysis of the 20/40 mesh sand was satisfactory as all samples fall within the primary and the secondary sieves. The bulk density of the sand is 1.64 g/cm$^3$, the Sphericity and roundness value of 0.8 was recorded for the sand. The loss on ignition (LOI) is in the range of 1.33% to 1.64%, while the sand has a hardness value of 8 on the Mohs scale. The XRF analysis showed that the sand is predominantly composed of oxides of Aluminium and Silicon ($Al_2O_3$ and $SiO_2$); while the acid solubility results showed a value of 0.7% for Luwa sand and 4.23% for the resin-coated sand. The turbidity value of 28.98 NTU was recorded for Luwa sand. This study is significant to the petroleum industry because it may succeed in the possible use of Luwa sand as proppant in hydraulic fracturing of hydrocarbon reservoirs. When considered as a commercial proppant, Luwa sand will generate revenue for the government because it will serve as a major commodity in the global proppant mix just as the Ottawa and Brady sands in the United States of America. Therefore, it is expected that government should encourage, assist and invest in the companies that will extract quality sand in Nigeria because of its large abundance in different parts of the country.

Future work on Luwa sand should include proppant conductivity test to determine the amount of hydrocarbon flow the proppant pack will permit.

**ACKNOWLEDGEMENTS**

The authors wish to thank the Petroleum Technology Development Fund (PTDF) for the construction of the PTDF building in Abubakar Tafawa Balewa University, Bauchi which housed the laboratory used for this study.

**REFERENCES**

[1] Abu Bakar, N., Zawawi, S., Zin, R., Rahman, N., Shaari, N., 2018. Characterization of Sand Proppant and its improvement via polyurethane coating. *International Journal of Engineering and Technology*, 7 (18) pp. 390 -399

[2] Al-Rbeawi, S., 2017. Analysis of pressure behaviours and flow regimes of naturally and hydraulically fractured unconventional gas reservoirs using multi-linear flow regimes approach. *Journal of Natural Gas Science and Engineering*, 45 (1) pp. 637-658.

[3] API RP 19C., 2008. Recommended practice for measurement of and specifications for proppants used in hydraulic fracturing and gravel-packing operations. *American Petroleum Institute.*

[4] Bandara, K., Ranjith, P., Zheng, W., Tennant, D., Silva, S., Rathnaweera, T., 2022. Grain-scale analysis of proppant crushing and embedment using calibrated discrete element models. *Acta Geotechnica*, 17 (1) pp. 4837-4864. https://doi.org/10.1007/s11440-022-01575-9.

[5] Conway, M., Lindeman, S., Barree, R., 2007. Selection of stimulation fluids and treatment design for low permeability reservoirs, *Presented at the SPE Hydraulic Fracturing Technology Conference, College Station, Texas, U.S.A.*

[6] Elochukwu, H., Kiat, K. (2020). Characterization of Baram and Tanjung sands as potential proppants. *Energy geoscience*. http://doi.org/10.1016/j.engeos.2020.12.002.

[7] Gu, M., Dao, E., Mohanty, K., 2015. Investigation of ultra-light weight proppant application in shale fracturing. *Fuel*, 150 (1), pp. 191-201.

[8] Guo, T., Zhang, S., Wang, L., Sui, W., Wen, H., 2012. Optimization of proppant size for frac pack completion using a new equipment. *Journal of Petroleum Science and Engineering*, 96 (1), pp.1-9.

[9] Ismail, S., Dahlila, K., Suhaila, M., 2011. Characterization of Malaysian Sand for Possible Use as Proppant. *American International Journal of Contemporary Research*, 1(1), pp.37-44.

[10] ISO 13503-2., 2006. Petroleum and natural gas industries - Completion fluids and materials – Part 2: Measurement of properties of proppants used in hydraulic fracturing and gravel-packing operations. *International Organization for Standardization (ISO).*

[11] Kaufman, P., Gupta, D., Richards A., 2015. Method of treating a subterranean formation with non-spherical proppants. US 9051512 B2.

[12] Kamel, A., Salem, Z., Chemini, R., Khodja, M., Allia, K., 2019. Characterization of natural sand proppant used in hydraulic fracturing fluids. *Particulate Science and Technology*, 37 (6), pp. 716-724. http://doi.org/10.1080/02726351.2018.1438542.

[13] Khair, E., Abdolla, O., Ahmed, M., Fathi, M., 2017. Feasibility Study of Bayuda's sand for Possible use as Proppant in Oil Field. *Oil and Gas research*, 3(2). http://doi.org/10.4172/2472-0518.1000137.

[14] Labus, K., Marga, R., Suponik, T., Maslowski, M., Wilk, K., Kasza, P., 2019. The concept of coke-based proppant for coal bed fracturing. *Earth and Environmental Sciences*.

[15] Liang, F., Sayed, M., Al-Muntasheri, G., Chang, F., Li L., 2016. A comprehensive review on proppant technologies. *Petroleum*, 2 (1) pp. 26–39.

[16] Liu, D., Yan, Y., Bai G., Yuan, Y., Zhu, T., Zhang, F., Shao, M., Tian, X., 2018. Mechanism for stabilizing and supporting shale fractures with nanoparticles in Pickering emulsion. *Journal of petroleum science and engineering*, 164, pp. 103 – 109.

[17] Mehmood, F., Liao, J., Hou, M., Zahoor, M., Xiong, Y. (2022). Optimization of hydraulic fracturing with rod-shaped proppants for improved recovery in tight gas reservoirs. *Geomechanics and Geophysics for Geo-Energy and Geo-resources*, 8(38) https://doi.org/10.1007/s40948-022-00347-9.

[18] Mocciaro, A., Lombardi, M., Scian N., 2018. Effect of raw material milling on ceramic proppants properties. *Applied clay science*, 153 (1) pp. 90-94.

[19] Palisch, T., Chapman, M., Leasure, J., 2015. Novel proppant surface treatment yields enhanced multiphase flow performance and improved hydraulic fracture clean-up. *Society of Petroleum Engineers*.

[20] Palisch, T., Saldungaray, P., 2013. Understanding Ceramic proppants: Are they all created equal? *CARBO ceramics Inc*.

[21] Palisch, T., Wilson, B., Duenckel, B., 2014. New technology yields ultra-high strength proppant. Presented in *Society of Petroleum Engineers Production and Operations*, 30 (1).

[22] Sun, H., He, B., Xu, H., Zhou, F., Zhang, M., Li, H., Yin, G., Chen, S., Xu, X., Li, B., 2022. Experimental Investigation on the Fracture Conductivity Behavior of Quartz Sand and Ceramic Mixed Proppants. *ASC Omega*,7 (1) pp. 10243 - 10254.

[23] Tang, Y., Ranjith, P., Perera, M., 2018. Major factors influencing proppant behaviour and proppant-associated damage mechanisms during hydraulic fracturing. *Acta Geotechnica*, 184 (4), pp. 757-780.

[24] Wahab, G., Ibrahim, G., Wahab, A., 2022. Geological and engineering appraisal of hydraulic

frac sand in some Egyptian localities as a proppant of oil well drilling. *Heliyon*. http://doi.org/10.1016/j.heliyon.2022.el0233.

[25] Wahab, G., and Ibrahim, G., 2021. Characterization of some Egyptian white sand and dunes for utilization for utilization as hydraulic fracturing sand for tight oil well layers. *Annuals geological survey*, *Egypt*, 38 (1).

[26] Xu, F., Yao, K., Li, D., Xu, D., Yang, H., 2022. Study on the Effect of Acid Corrosion on Proppant Properties. *Energies*, 15 (1). http://doi.org/10.3390/en15228368.

[27] Zheng, W., Silva, S., and Tannant, D., 2017. Crushing characteristics of four different proppants and implications for fracture conductivity. *Journal of Natural Gas Science and Engineering*, 53(1) pp.355-361.

[28] Zoveidavianpoor, M., Gharibi, A. (2016). Characterization of agro-waste resources for potential use as proppant in hydraulic fracturing. *Journal of natural gas science and engineering*, 53 (1) pp. 355-361.

[29] Zoveidavianpoor, M., Gharibi, A., Farokhi, M., Nasef, M., 2014. Low weight composite proppant for hydraulic fracturing of subterraneous formation: Experimental analysis. *Presented at the 4th international Conference on* Composites: Characterization, Fabrication and Application, Iran University of Science and Technology, Tehran, Iran.